Delft Wood Science Foundation Publication Series 2006, nr. 3 - ISSN 1871-675X

Derivation of the bearing strength perpendicular to the grain of locally loaded timber blocks.

Based on the equilibrium method of plasticity, the theoretical explanation of the bearing strengths of locally loaded blocks is given in the Appendices.
The result of the numerical construction of the slip-lines can precisely be represented by an analytical function as logarithmic spiral that can be shown to be the exact solution. This function can be given in the power law form leading to a theoretical and experimental value of the power of 0.5.
This power representation of the stress spreading model of confined dilatation provides a simple design method that precisely matches to the data in all circumstances and loading cases and explains the apparent contradictory test results of Suenson, the Eurocode, the French rules, Graf, Korin and Augustin et al

dr. ir. T.A.C.M. van der Put

of the
Delft Wood Science Foundation
em. assoc. Research Professor of the
Technical University of Delft

DelftWoodScienceFoundation@xs4all.nl

Wielengahof 16
NL 2625 LJ Delft

Tel. +31152851980

Bearing strength perpendicular to the grain of locally loaded blocks

The local compression strength perpendicular to the grain may increase due to confined dilatation perpendicular to the loading direction. This is explained in Appendix A by the equilibrium method of the theory of plasticity. As derived, the increase of strength is proportional with $\sqrt{L/s}$ according to Eq.(1).

$$f_{c,s} = c \cdot f_{c,90} \cdot \sqrt{L/s} = 1.08 \cdot f_{c,90} \cdot \sqrt{L/s} \qquad (1)$$

The definition of L and s is given in Fig. 2.

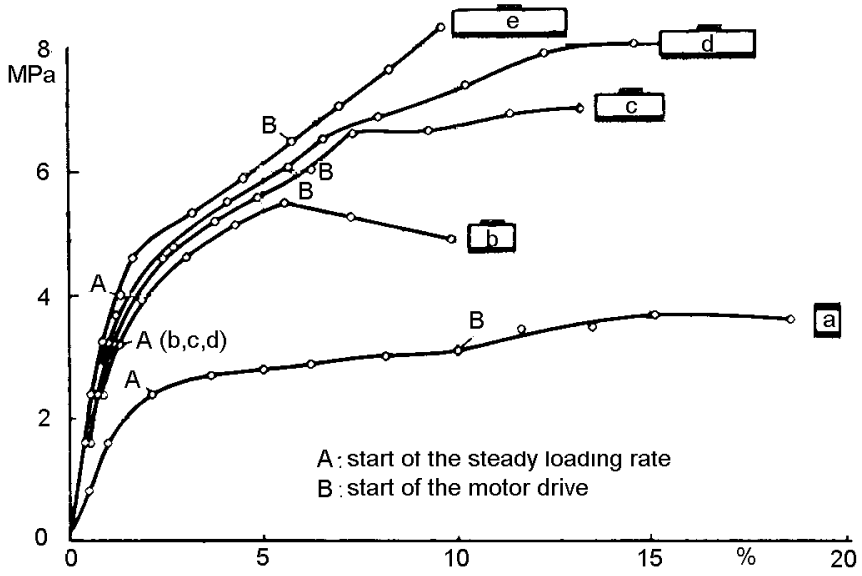

Fig. 1 - Bearing strength $f_{c,s}$ perpendicular to the grain. Specimen 15x15 cm, lengths: L = 15, 30, 45, 60, 75 cm, of curve a to e, [1] Suenson. s = 15 cm.

The strength values $f_{c,s}$ are the top-values of the measured curves of Fig. 1. The compression strength $f_{c,90}$, at the top of curve "a" at 15% strain, is here 3.6 MPa.

Table 1 – Bearing strengths perpendicular to the grain of locally loaded blocks

Curve	L/s	$\sqrt{L/s}$	$f_{c,90}$ MPa	Theory $f_{c,s} = 1.1 \cdot f_{c,90} \sqrt{L/s}$ MPa	Measurements $f_{c,s}$ MPa	ultimate strain
a	1	1	3.63	$1.1 \cdot f_{c,90} = 4.0$		15%
b	2	√2		5.6	5.5	5.5%
c	3	√3		6.9	6.95	13%
d	4	√4		8.0	8.0	15%
e	5	√5	limit	≈ as curve "d"	8.3	10%

The measured maximal strength values, given in Table 1, are precisely according to the theory. Fig. 1 shows the strength increase with the increasing possibility of

spreading of the load. It further shows that there is a maximal spreading of about 4H because the strengths of block "e" and "d" are equal. The strength of specimen "e" with L = 5s = 5H, is as strong as specimen "d" with L = 4s = 4H. The definition of L, s and H is given in Figure 2. The maximal spreading-length thus is 4H, or better is: 3H + s. Because s = H, the spreading is 3H, thus 2 times 1.5·H of both sides. Thus L = 2·1.5·H + s = 3H + H = 4H. The spreading thus is 1.5:1, as is applied in fig.5.
When the ultimate state is chosen at a small plastic deformation, as often done, the spreading slope is close to 1:1 of the elastic state. This also is to be expected when there is no friction at the bearing plates or when not the height H is limiting but the spreading length L is limiting being equal then to the length of the block. On this determining case the derivation of Eq.(A.17) from Eq.(A.13) is based in Appendix A.
The same maximal value of the spreading slope of 1.5:1 also follows from other investigations as e.g. given in Table 2 of the French design rules where also for higher values of "a" above a/H ≥ 1.5 there is no strength increase.
Eq.(1) provides a simple design rule and is able to explain all mutual strongly different empirical results, as will be discussed here.
The rule of the Eurocode, given in [5], Eq.(4.20), follows from Eq.(1). Because $f_{c,s} = f_{c,90}\sqrt{L/s}$ and $f_{c,s,0} = f_{c,90}\sqrt{L/s_0}$, is:

$$f_{c,s} / f_{c,s,0} = \sqrt{s_0 / s} = (s_0 / s)^{0.5}. \qquad (2)$$

This equation is chosen to apply for $s \le s_0 = 100$ mm and in [5], the exponent 0.5 is replaced by 0.4, to better follow the existing safe Code rules of Canada, Denmark, Norway Sweden and the UK. This however, only is the case for 100 ≥ s ≥ 50 mm. For s ≤ 50 mm, the curve lies increasingly above these Code values. This was corrected for small values of s in the CIB – Timber Code by choosing a power of 0.25 while wrongly $f_{c,s,0}$ was taken to be equal to $f_{c,90}$ for $s = s_0 = 150$ mm. Because L and thus H are eliminated in the derivation of Eq.(2), the equation is not general applicable. For very small values of H for instance, there is no spreading at all and the equation doesn't apply. Therefore the right rule, based on the theoretical Eq.(1) was proposed for the Timber Code several times in the past as e.g. in [8] and [9].

Table 2 – Values of $k_c = fc_{c,s} / f_{c,90}$

s/H	a/H			
	≥ 1.5	1	0.5	0
1	2	1.5	1.25	1
2	1.5	1.25	1.12	1
≥ 3	1	1	1	1

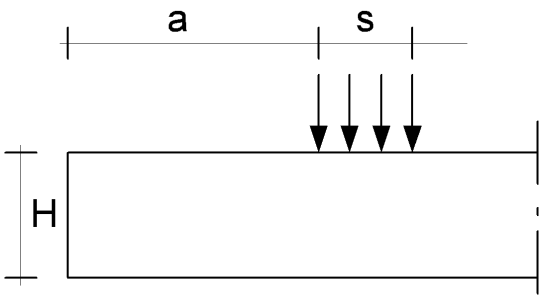

Fig. 2 – Locally loaded Block

The French rules, given in Table 2, mentioned in [5], correct for the omission of H in the CIB Code by showing the dependence of the strength on H. The table shows the boundary value of a/H = 1.5, mentioned above. When a/H = (L - s)/2H ≥ 1.5, thus when L ≥ 3H + s, the maximal spreading is reached according to Fig. 1. An other boundary of the table is given for s/H ≥ 3. It then is assumed that in the middle of the specimen the same conditions appear as in the cube test. This applies for fully flexible, frictionless bearing plates.

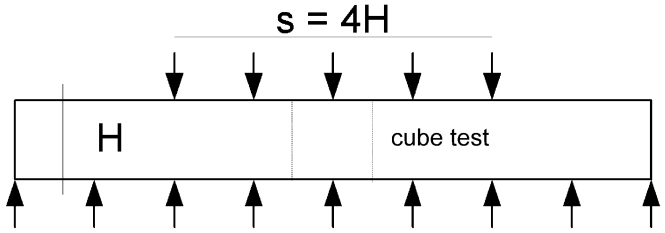

Fig. 3 -Cube test condition in the middle when there is no friction.

The same condition is assumed to apply for a = 0 in fig. 2. Without friction, spreading is not possible at the edge and the strength is equal to the strength of the cube test. With friction along the plates, the confined pressure may e.g. be build up, even for s = L, according to Fig. 4.

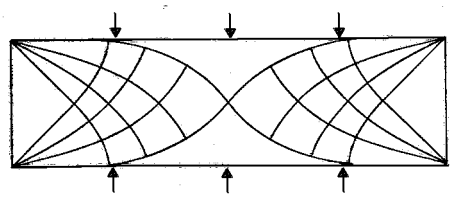

Fig. 4 – Slip lines of failure between two plates by friction along the plates.

The influence of no friction along the bearing plate in the strong direction (and thus full friction in the width direction) can be assessed as lower bound by assuming that only symmetrical spreading is possible. Thus for Table 2 and 3: L = 2a + s.
According to Eq.(1) then is: $k_c = \sqrt{L/s} = \sqrt{1+(2a/H)/(s/H)}$ in Table 3.

Table 3 – Values of $k_c = f_{c,s} / f_{c,90}$

s/H	a/H = (L – s)/2H			
	≥ 1.5	1	0.5	0
1	2	1.7	1.4	1
2	1.6	1.4	1.2	1
≥ 3	1	1	1	1

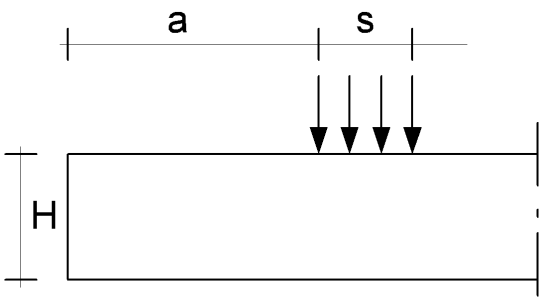

These values are close to the values of Table 2 and are comparable when:

$$0.9 \cdot \begin{pmatrix} 1.7 & 1.4 \\ 1.4 & 1.2 \end{pmatrix} = \begin{pmatrix} 1.5 & 1.25 \\ 1.25 & 1.1 \end{pmatrix}.$$

Thus when, outer c = 1 in the first column, c = 0.9 in column 2 and 3 is used, indicating the safe lower bounds given by the French rules.

In [6], test results are given of bearing in the range where H is not limiting for spreading because: L < 2H + s in the central loaded specimen. The determination of $f_{c,90}$ is done on the same specimen, thus on the specimen of fig. 5 with an upper loading plate of length L, the same length as the bottom plate, giving by this form a higher strength than follows from the common compression test. The ultimate strain was chosen to be 2.5 %.

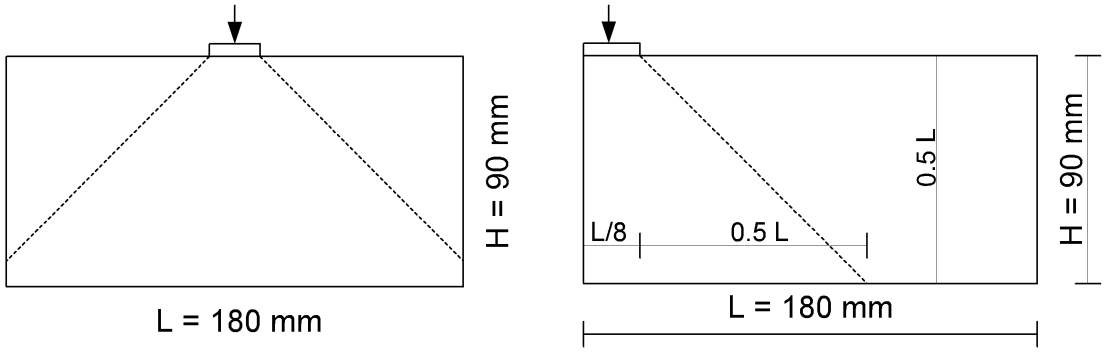

Fig. 5 -- Spreading 1:1 in a central loaded block and end-loaded block of [6].

Table 4 – Values of k_c according to the test-specimens of fig.5.

	measurements		Theory	
s/L	central Loaded k_c	end loaded k_c	central loaded Eq.(1): $k_c = \sqrt{L/s}$	end loaded
1	1	1	1	1
0.875	1.063	1.063	$\sqrt{1/0.875} = 1.07$	$\sqrt{1/0.875} = 1.07$
0.75	1.188	1.156	$\sqrt{1/0.75} = 1.16$	$\sqrt{1/0.75} = 1.16$
0.625	1.375	1.281	$\sqrt{1/0.625} = 1.27$	$\sqrt{1/0.625} = 1.27$
0.5	1.625	1.438	$\sqrt{1/0.5} = 1.41$	$\sqrt{(0.5+0.5)/0.5} = 1.41$
0.375	1.969	1.625	$\sqrt{1/0.375} = 1.63$	$\sqrt{(0.375+0.5)/0.375} = 1.53$
0.25	2.344	1.875	$\sqrt{1/0.25} = 2$	$\sqrt{(0.5+0.25)/0.25} = 1.73$
0.125	2.781	2.156	$\sqrt{L/0.125L} = 2.8$	$\sqrt{(0.5+0.125)/0.125} = 2.2$

This compression strength is compared in [6] with the strength of the ASTM-bearing test, being the same test as given by the central loaded specimen of fig. 5, however

with a length of the upper plate of L/3. This explains why in the graph in [6] of the ASTM values are $\sqrt{L/s} = \sqrt{3}$ times higher than according to the compression strength of [6] done on the same specimen with s = L.
In table 4 the test results (of series of 3 specimens) are compared with Eq.(1) and it is seen that also non-symmetrical spreading is possible of end loaded blocks because of the friction between plate and specimen
According to the Eurocode a limiting value occurs at $s/L \leq 0.125$ due to a local mechanism. The results here however don't show such an empirical reduction of the strength with respect to the theoretical value. Also the theoretical limit values of the local mechanisms show much higher values of k_c.
In table 5, the empirical value of c of eq.(1) is given, based on the tests of [6].

Table 5 – Values of $f_s / f_{c,90} = k_c$ and of $c = k_c / \sqrt{L/s}$, according to Table 4.

	Measurements		Theory $k_c = \sqrt{L/s}$			
s/L	central loaded k_c	end - loaded k_c	central loaded k_c	end loaded k_c	c-values of Eq.(1) $c = k_c/\sqrt{L/s}$	$= k_c/\sqrt{L/s}$
1	1	1	1	1	1	1
0.785	1.063	1.063	1.07	1.07	1	1
0.75	1.188	1.156	1.16	1.16	1.03	1
0.625	1.375	1.281	1.27	1.27	1.09	1
0.5	1.625	1.438	1.41	1.41	1.15	1
0.375	1.969	1.625	1.63	1.53	1.2	1.06
0.25	2.344	1.875	2.0	1.73	1.17	1.08
0.125	2.781	2.156	2.8	2.2	1	1 limit
mean of c:					1.08	1

In Fig. 6, the results are given of tests on two sided locally loaded long blocks.
From the figure it follows that: $s + 3\alpha H = L + 3.(1 - \alpha)H$. Thus:

$$\alpha = 0.5 + \frac{L - s}{6H}$$

and thus the equivalent spreading factor (of the strength determining plate) is:

$$\frac{L'}{s} = \frac{s + 3\alpha H}{s} = 1 + \frac{3H}{s}\left(0.5 + \frac{L - s}{6H}\right) = 0.5 + \frac{3H + L}{2s}$$

With H = 17.9; L = 35 and b = 18.1 cm according to the measurements of O. Graf is:

$$k_{c,90} = c \cdot \sqrt{\frac{L'}{s}} = 1.1 \cdot \sqrt{0.5 + \frac{3H + L}{2s}}$$

or: $k_{c,90} = 1.1 \cdot \sqrt{0.5 + (3 \cdot 17.8 + 35)/2s} = 1.1 \cdot \sqrt{0.5 + 44.2/s}$

leading to the values of f_s at 5 mm deformation (see figure) of the curves:
1: 16 - 2: 30 - 3: 36 - 5: 43 - 6: 52 kgf/cm², about the same as the measurements as can be seen in Table 6.

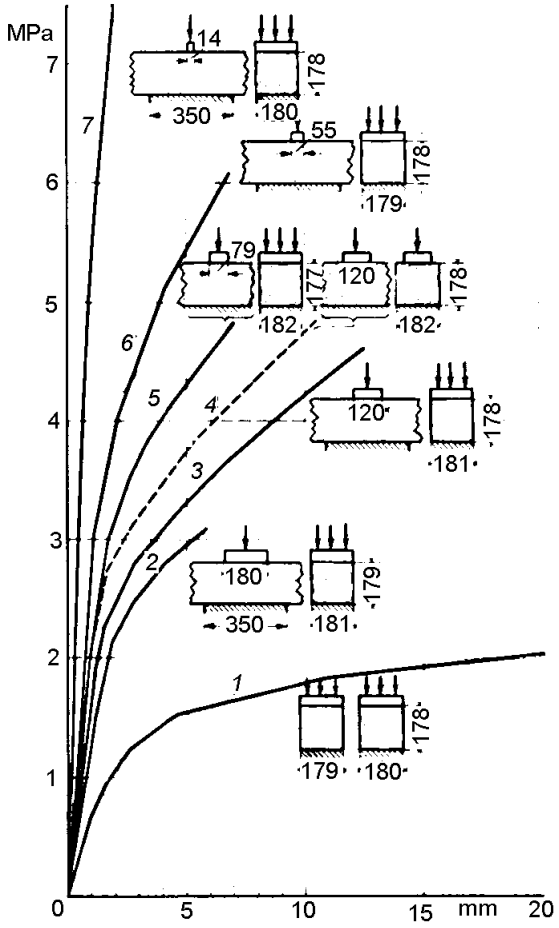

For long blocks with respect to the bearing plates the maximal spreading will occur at both plates according to the figure 6..

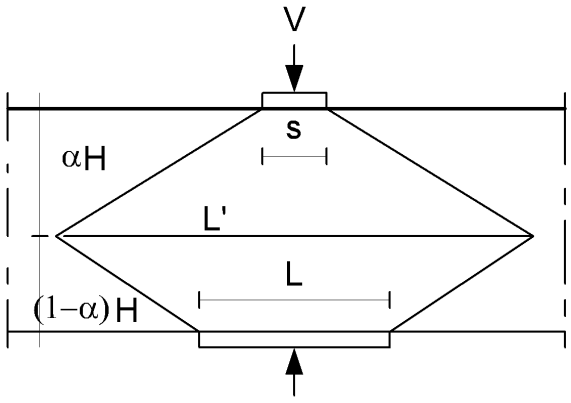

Fig. 6 - Local loading perpendicular to the grain [1] Graf

Table 6 - $k_{c,90} = f_s / f_{c,90} = 1.1 \cdot \sqrt{0.5 + 44.2/s}$

Curve	s cm	$f_{c,90}$ MPa	$k_{c,90}$	Theory f_s MPa	Measurements f_s MPa	ultimate strain 6/178 or: 3.4%
1	18	1.6		1.6	1.6	3.4%
2	18		1.89	3.0	3.0	3.4%
3	12		2.25	3.6	3.3	3.4%
5	7.9		2.72	4.3	4.3	3.4%
6	5.5		3.21	5.2	5.4	3.4%
7	1.4		6.23	10 or local limit	> 7.5	> 1%

The highest maximum is not shown (of line 7 of fig.6). Predicted according to the last formula is: f_s = 10 MPa. However this may be cut off by a local mechanism. Because $f_s \geq 7.5$ MPa is measured, the maximum value of $k_{c,90}$ is at least 7.5/1.6 = 4.7, near the

theoretical value obtained from a local failure mechanism (giving an upper bound value) of about 5.5 to 6).
The measurements of fig. 6 suggest a constant loading rate with a sudden instability of the test at the end. Therefore the curves 2, 5 and 6 end early at about 6 mm or 3.4% strain. For this reason all strengths were defined at this strain.
The theoretical explanation of the test results of [7] is discussed next. This still appears to be necessary although the theory was published long ago and is applied in many reports of the Stevin Laboratory as e.g. in [10], where it is shown to be the only possible theory to explain the very high embedding strengths of particle board in compression.
The theory also is published in CIB-papers e.g. in [8] and in a report for the CIB-Stability Committee and more recently in [9], where it a was shown that the theory fully and precisely explains the data of Ballerini of [11] and the Karlsruher data of joints with one dowel.
According to the theory Eq.(1) applies for the compression strength perpendicular to the grain, of a locally loaded bearing block:

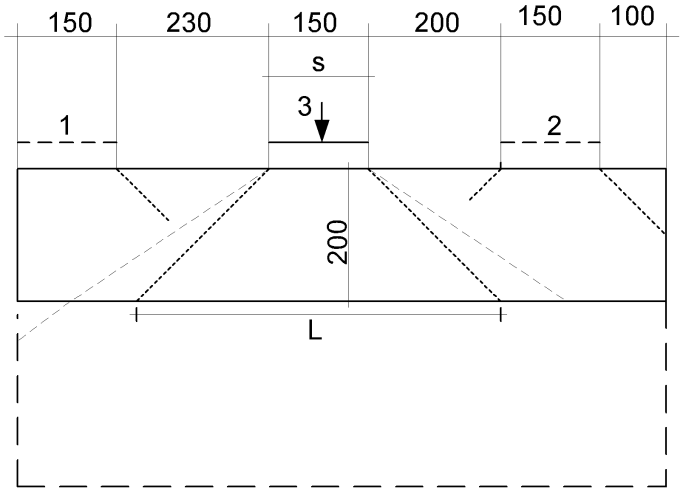

Fig. 7 – Test specimen of [7]

The factor of the increase of the compression strength by local loading k_c thus is:

$$k_c = f_{lc,90} / f_{c,90} = \sqrt{L/s}$$

Because the 1% permanent strain (≈ 3% total strain) is chosen as ultimate strain, the stress distribution will be close to the elastic one and a spreading of about 1 to 1, or 45^0 can be assumed (see Fig. 7). The maximal spreading at higher strains will be 1.5 to 1. The length L thus will be for case 1 of Fig. 1, L = 200α + 150. For case 2 is: L = 200α + 150 + 100, and for case 3: L = 2α·200 + 150 mm, where α = 1 to 1.5. The length s = 150. For the specimen height of 480 mm, all values of 200 in the expressions of L should be replaced by 480.
Thus:
case 1: $k_c = \sqrt{L/s} = \sqrt{(200+150)/150} = 1.53$ to $\sqrt{(1.5\cdot 200+150)/150} = 1.73$, etc.

For case 3 with H = 480, L can not be higher than the length of the specimen of 980 mm and thus this length is the real spreading length giving $k_c = \sqrt{980/150} = 2.56$.

Table 1 – Empirical verification of the theoretical values of k_c.

$k_c = \sqrt{L/s}$	theory, 1% strain $\alpha = 1$	measurements 1% strain	theory, prediction for high strain $\alpha = 1.5$
h = 200 mm case 1 case 2 case 3	k_c = 1.53 = 1.73 = 1.91	k_c = 1.58 = 1.94 = 1.94	k_c = 1.73 = 1.92 = 2.24
h = 480 mm case 1 case 2 case 3	k_c = 2.05 = 2.21 = 2.56	k_c = 1.82 = 2.12 = 2.46	k_c = 2.41 = 2.54 = 2.56

It can be seen that the measurements are close to the applied low strain prediction of the theory with the spreading slope of 45^0, giving a very good explanation of the data at the different configurations. The higher strain predictions of the theory should be verified.

It can be concluded that the theory gives an excellent explanation and precise fit of all the apparent contradictory test results of Suenson, the Eurocode, the French rules, Graf, Korin and Augustin et al. in all circumstances and loading cases.
Therefore the proposal of the past remains to use the right design rules as for the Codes as given below.
As proposal for the Eurocode the following rules are possible for bearing blocks:
$\sigma_{c,90,d} \le k_{c,90} \cdot f_{c,90,d}$, where:
$k_{c,90} = \sqrt{L/s}$ with: $L \le a + s + l_1/2$; $L \le 3H + s$ and:
$k_{c,90} = 2.8$ when $s/L \le 0.125$ for central loads;
$k_{c,90} = 2$ when $s/L \le 0.25$ for end loads.
For safe rules (when friction is only in the width direction), the conditions are:
$L \le 2a + s$; $L \le s + l_1$; $L \le 2H + s$,
$k_{c,90} = 2.8$ when $s/L \le 0.125$
For the bearing strength of a middle section of a beam between two plates of lengths L and s is:

$$k_{c,90} = 1.1 \cdot \sqrt{0.5 + \frac{3H + L}{2s}} \le 5$$

These rules for bearing block don't apply for support stresses of beams. For the combined stresses in the beam, the failure criterion of [4] has to be applied. As long

this exact approach is not followed, the compression strength perpendicular to the grain at a middle support should safely be limited to $f_{c,90}/2$ in order to maintain the ultimate compression stress of the bending strength of the beam.

Appendix A

Derivation of the bearing strength perpendicular to the grain or locally loaded blocks and of the spreading equation by the method of characteristics

The dependence of the strength upon spreading can be explained by the equilibrium method of the theory of plasticity. In the plastic region, a stress field can be constructed in the specimen that satisfies the equilibrium conditions:

$$\frac{\partial \sigma_x}{\partial x}+\frac{\partial \tau}{\partial y}=0 \quad \text{and} \quad \frac{\partial \tau}{\partial x}+\frac{\partial \sigma_y}{\partial y}=0 \tag{A.1}$$

and the boundary conditions and nowhere surmounts the failure criterion.
For this mostly determining failure criterion an inscribed Tresca criterion, Eq.(A.2), can safely be used

$$(\sigma_1-\sigma_2)/2=k=f_v \tag{A.2}$$

This failure criterion applies after a flow and hardening stage in the weak directions until a quasi isotropic flow behaviour occurs followed by further hardening ([2], [4]) and flow. In the figure below, a Mohr-circle of the failure condition is given with the general stress state σ_x, σ_y, τ. In Fig. A.1 is:

$$p=(\sigma_1+\sigma_2)/2 \quad \text{and} \quad k=(\sigma_1-\sigma_2)/2. \tag{A.3}$$

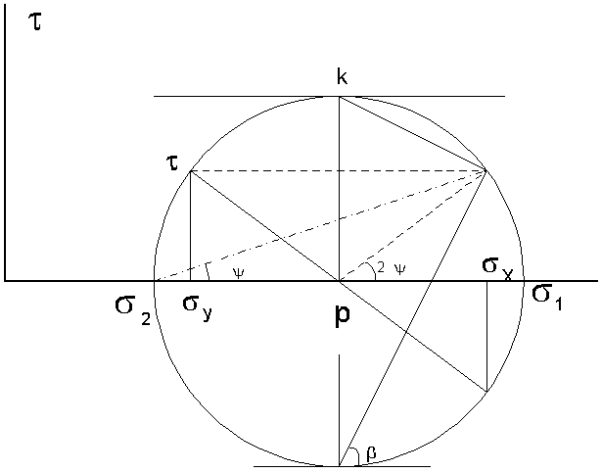

Fig. A.1 – Tresca failure condition

In general is: $p=\sigma_y+k\cos 2\psi=\sigma_x-k\cos 2\psi$ and $\tau=k\sin 2\psi$

Substitution of these equations of σ_x, σ_y, τ in the equilibrium equations gives

$$\frac{\partial p}{\partial x}-2k\sin 2\psi\frac{\partial \psi}{\partial x}+2k\cos 2\psi\frac{\partial \psi}{\partial y}=0 \tag{A.4}$$

$$\frac{\partial p}{\partial y} + 2k\cos 2\psi \frac{\partial \psi}{\partial x} + 2k\sin 2\psi \frac{\partial \psi}{\partial y} = 0 \qquad \text{(A.5)}$$

Multiplication of Eq.(5) by tan($\psi - \pi/4$) and then addition with Eq.(4) gives:

$$\frac{\partial a}{\partial x} + \tan(\psi - \pi/4) \cdot \frac{\partial a}{\partial y} = 0 \qquad \text{(A.6)}$$

where $a = p - 2k\psi$. Thus along the characteristic with slope dy/dx = tan($\psi - \pi/4$), is a = constant. The same can be done by multiplication of tan($\psi + \pi/4$), leading to

$$\frac{\partial b}{\partial x} + \tan(\psi + \pi/4) \cdot \frac{\partial b}{\partial y} = 0 \qquad \text{(A.7)}$$

giving $b = p + 2k\psi$ = constant along the characteristic with dy/dx = tan($\psi + \pi/4$), To show that these lines are characteristics, Eq.(4) and (5) are combined with their corresponding equations of variation:

$$\begin{pmatrix} 1 & 0 & -2k\sin 2\psi & 2k\cos 2\psi \\ 0 & 1 & 2k\cos 2\psi & 2k\sin 2\psi \\ 1 & \frac{dy}{dx} & 0 & 0 \\ 0 & 0 & 1 & \frac{dy}{dx} \end{pmatrix} \begin{pmatrix} \partial p/\partial x \\ \partial p/\partial y \\ \partial \psi/\partial x \\ \partial \psi/\partial y \end{pmatrix} = \begin{pmatrix} 0 \\ 0 \\ dp/dx \\ d\psi/dx \end{pmatrix}$$

In this region in the failable state, lines can be given along which failure is initiated corresponding to the initiation of motion. Accordingly these are lines, called characteristics, across which derivatives may become discontinuous, or along which discontinuities in derivatives may propagate. On these lines, in the characteristic directions the derivatives thus have no determinate value and the directions can be found by equating all determinants to zero. A zero value of the nominator determinant gives, after subtraction of the third row from the first:

$$\det \begin{pmatrix} -\frac{dy}{dx} & -2k\sin 2\psi & 2k\cos 2\psi \\ 1 & 2k\cos 2\psi & 2k\sin 2\psi \\ 0 & 1 & \frac{dy}{dx} \end{pmatrix} = 0$$

or

$$-\left(\frac{dy}{dx}\right)^2 \cos 2\psi + 2\left(\frac{dy}{dx}\right)\sin 2\psi + \cos 2\psi = 0 \quad \text{or:} \quad \frac{dy}{dx} = \tan 2\psi \pm \sec 2\psi \quad \text{or:}$$

$$\frac{dy}{dx} = \tan\left(\psi + \frac{\pi}{4}\right) \qquad \text{and} \qquad \frac{dy}{dx} = \tan\left(\psi - \frac{\pi}{4}\right) \qquad \text{(A.8)}$$

This thus are the slopes of both orthogonal characteristics.

A zero value of the denominator determinant gives:

$$\det\begin{pmatrix} -\frac{dy}{dx} & -2k\sin 2\psi & -\frac{dp}{dx} \\ 1 & 2k\cos 2\psi & 0 \\ 0 & 1 & \frac{d\psi}{dx} \end{pmatrix} = 0 \text{ or } -\frac{dy}{dx}\left(\frac{d\psi}{dx}\cos 2\psi\right) + \frac{d\psi}{dx}\sin 2\psi - \frac{1}{2k}\frac{dp}{dx} = 0$$

or with the found equation above of dy/dx :

$$-\left[(\tan 2\psi \pm \sec 2\psi)\cos 2\psi - \sin 2\psi\right]\cdot\frac{d\psi}{dx} - \frac{1}{2k}\frac{dp}{dx} = 0 \quad \text{or:} \quad \pm\frac{d\psi}{dx} - \frac{1}{2k}\frac{dp}{dx} = 0 \quad \text{or:}$$

$$p - 2k\psi = a = \text{constant} \tag{A.9}$$

$$p + 2k\psi = b = \text{constant} \tag{A.10}$$

along the first respectively the second characteristic (as found before).
Calculation of the network of these slip-lines is done numerically. From two

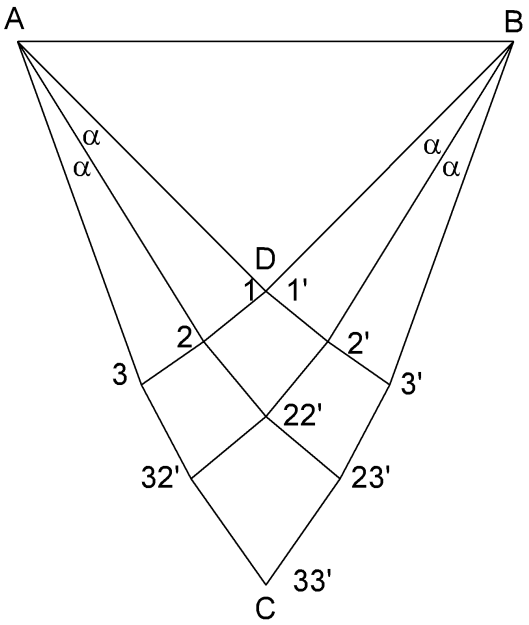

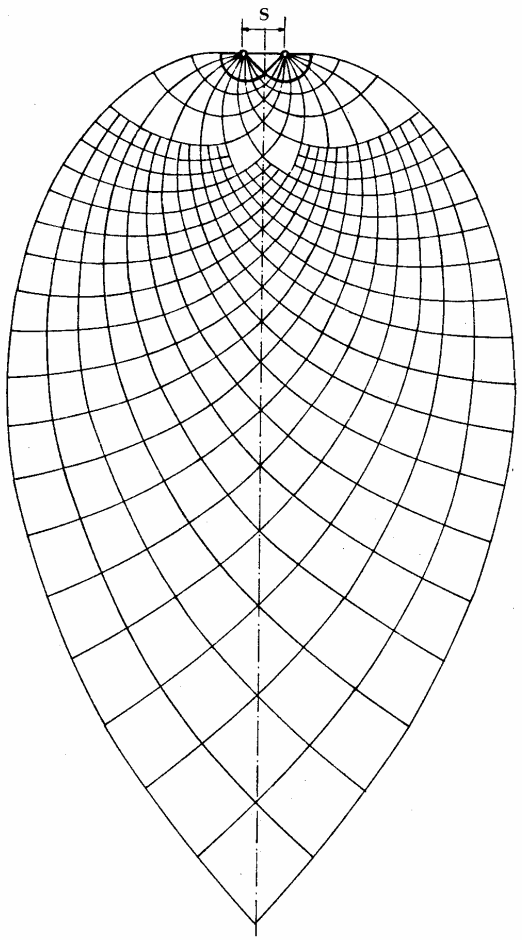

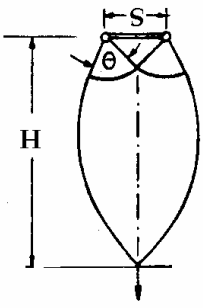

Fig. A.2 - Construction of the slip lines.

known points, known from the boundary condition or previous calculation, x_1, y_1 and x_2, y_2, the next point x, y follows from:

$$y - y_1 = (x - x_1)\cdot\tan(\psi - \pi/4) \quad \text{and} \quad y - y_2 = (x - x_2)\cdot\tan(\psi + \pi/4)$$

or after elimination of the unknowns:

$$x = \frac{x_1 \tan(\psi_1 - \pi/4) - y_1 - x_2 \tan(\psi_2 + \pi/4) + y_2}{\tan(\psi_1 - \pi/4) - \tan(\psi_2 + \pi/4)} \quad \text{and} \quad y = y_2 + (x - x_2)\tan(\psi_2 + \pi/4)$$

The value of ψ follows from (b – a)/2 of point 1 and 2, and p follows from (a + b)/2. The result of the numerical construction of the slip-lines, given in [3] and Fig. A.2, can be precisely approximated by the function:

$$\theta \approx 0.62 \cdot \ln(2H/s) \qquad \text{(A.11)}$$

This can be explained as follows. At the end of the outer curved slip-line over a length $Rd\phi$ is according to the chain equation $Nd\phi = \sigma Rd\phi$ or $N = \sigma R$, where N is the normal force along the slip-line. Further is also $dN = \tau Rd\phi$, or $\sigma\, dR = \tau Rd\phi$, or $d(\ln R)/d\phi = \tau/\sigma = \mu$ and thus $R = R_0 \exp(\mu\phi)$, what is a logarithmic spiral. Now is:

$$\frac{R_L}{R_s} = \frac{H}{s/2} = \exp\left(c(\theta_L - \theta_s)\right) = \exp\left(1.61 \cdot \theta_t\right) \text{ or: } \theta_t \approx 0.62 \cdot \ln(2H/s).$$

It thus is probable that Eq.(A.11) is not an approximation but the true solution for the end point of the outer slip-lines.

Triangle ABD of Fig. 2 is a region of constant state, where the maximum shear lines, or characteristics, are everywhere at 45^0 to the principal directions because of the uniform compression load on plane AB. Because the pole of the planes in the Mohr circle now is at point σ_2 in Fig. A.1, is $\psi = \pi/2$. This direction of the plane with the minor principle stress is also the direction of the highest principle compression stress.

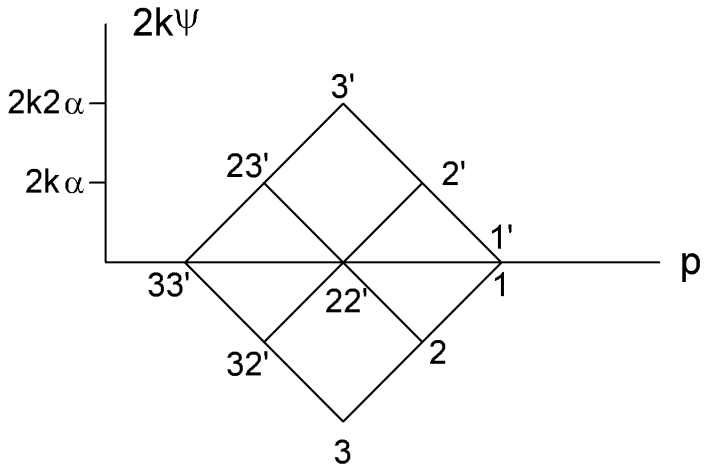

Fig. A.3 – Determination of p and ψ in the p – 2kψ plane

From point D, or point 11′ in Fig.A.2, to point 2., is:

$$p_s - 2k\frac{\pi}{2} = p_{2'} - 2k\left(\frac{\pi}{2} + \alpha\right). \text{ Thus: } p_{2'} = p_s - 2k\alpha$$

From point 2′ to 22′ is:

$$p_{22'} + 2k\frac{\pi}{2} = p_{2'} + 2k\left(\frac{\pi}{2} - \alpha\right). \text{ Thus: } p_{22'} = p_{2'} - 2k\alpha = p_s - 4k\alpha \text{ and: } p_s = p_o + 4k\alpha.$$

The same relation follows for point 33′, when the angle between line BD, and BC (at

point B) is 2α: $p_s = p_o + 4k(2\alpha)$. Thus in general is:

$$p_s = p_o + 4k\theta \qquad \text{(A.12)}$$

Inserting Eq.(A.11) and with $p_s = (\sigma_s + \sigma_s - 2k)/2 = \sigma_s - k$ and $p_o = \sigma_o - k$, this is:

$$\sigma_s = \sigma_o + 2.48 \cdot k \cdot \ln(2H/s) \qquad \text{(A.13)}$$

and because $\sigma_s \cdot s = \sigma_o \cdot L$ (see Fig. A.4) is: $\sigma_s(1 - s/L) = 2.48 \cdot k \cdot \ln(2H/s)$. Further elastic spreading will be at an angle of 45^0, thus for first flow, L ≈ 2H + s, or:
H ≈ (L - s)/2 when H > s, thus: L/s > 3
Substitution of the values for σ_0 and H in Eq.(A.13) gives:

$$\sigma_s = 2.48 \cdot k \cdot \ln\left(\frac{L}{s} - 1\right) \cdot \frac{L/s}{L/s - 1} \cdot \qquad \text{(A.14)}$$

and because from the power law approximation follows that $\ln\left(\frac{L}{s} - 1\right) \cdot \frac{L/s}{L/s - 1}$ is proportional to $\sqrt{L/s}$, (see Appendix B and C), Eq.(A.14) becomes:

$$\sigma_s = 2.48 \cdot k \cdot C \cdot \sqrt{L/s} \qquad \text{(A.15)}$$

where C is a about 0.78.
Thus:

$$\sigma_s = 0.97 \cdot 2k \cdot \sqrt{L/s} \approx 2k \cdot \sqrt{L/s} \qquad \text{(A.16)}$$

The value of k follows from the compression test (cube test) with $\sigma_1 = f_{c,90}$ and $\sigma_2 = 0$ or: $k = f_{c,90}/2$. Thus Eq.(6) becomes:

$$f_s = c \cdot f_{c,90} \cdot \sqrt{L/s} \approx f_{c,90} \cdot \sqrt{L/s} \qquad \text{(A.17)}$$

The higher experimental value of c given in Eq.(1) shows the lower bound approach of the chosen method (the real slip/lines must give a higher value). Thus c gives the possibility to adapt the model to test results.

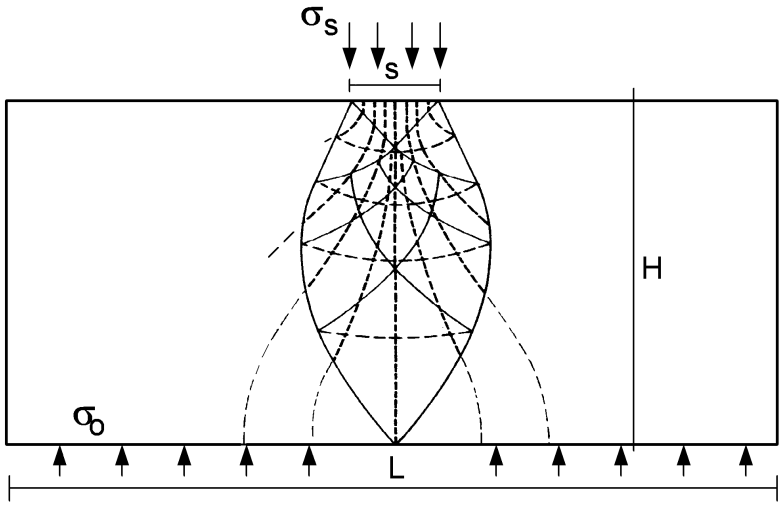

Fig. A.4. - "Slip-lines" determining the direction of the main stresses

A similar solution is possible for the rotational symmetrical case, leading to the extension of Eq.(A.17) to the surfaces A_s $(\pi s^2/4)$ and A_L $(\pi L^2/4)$. Thus generalized to every surface form:

$$f_s = c \cdot f_{c,90} \cdot \sqrt{A_L / A_s} \qquad (A.18)$$

Appendix B

Derivation of the power law.

Any function f(x) always can be written in a reduced variable x/x_0

$f(x) = f_1(x/x_0)$

and can be given in the power of a function:

$f(x) = f_1(x/x_0) = [\{f_1(x/x_0)\}^{1/n}]^n$ and expanded into the row:

$$f(x) = f(x_0) + \frac{x - x_0}{1!} \cdot f'(x_0) + \frac{(x - x_0)^2}{2!} \cdot f''(x_0) + ...$$

giving:

$$f(x) = \left[\{f_1(1)\}^{1/n} + \frac{x - x_0}{x_0} \frac{1}{n} \{f_1(1)\}^{1/n-1} \cdot f'(1) + ... \right]^n = f_1(1) \cdot \left(\frac{x}{x_0} \right)^n$$

when: $(f_1(1))^{1/n} = (f_1(1))^{1/n-1} \cdot f_1'(1)/n$ or: $n = f_1'(1)/f_1(1)$

where: $f_1'(1) = [\partial f_1(x/x_0)/\partial(x/x_0)]$ for $x = x_0$ and $f_1(1) = f(x_0)$

Thus: $$f(x) = f(x_0) \cdot \left(\frac{x}{x_0} \right)^n \quad \text{with} \quad n = \frac{f_1'(1)}{f_1(1)} = \frac{f'(x_0)}{f(x_0)} \qquad (B.1)$$

It is seen from this derivation of the power law, Eq.(B.1), using only the first two expanded terms, that the equation only applies in a limited range of x around x_0.

Appendix C

Derivation of the power of the spreading equation.

The in the Appendix A found part of Eq.(A.14): $(1.24 \cdot (L/s) \cdot \ln(L/s-1))/(L/s - 1)$, appears to follow the form of $\sqrt{L/s}$. This follows from the power law approximation of Eq.(A.14) (according to Appendix B) giving a power 0.5. It thus is possible to split Eq.(A.14) into: $\sqrt{L/s} \cdot (1.24 \cdot (\sqrt{L/s}) \cdot \ln(L/s-1))/(L/s - 1) = \sqrt{L/s} \cdot C$, because the second part should be about constant.

The special value of 0.5 of the power can be explained as follows. In the following derivation, the strengths of the upper and bottom planes will be related to the strength of an intermediate plane "m·e", having a strength according to the power law representation:

$\sigma_m = \sigma_c \left(\frac{Lt}{me}\right)^n$. Thus from: $\sigma_m me = \sigma_L Lt \rightarrow \sigma_L = \sigma_m \frac{me}{Lt} = \sigma_c \left(\frac{me}{Lt}\right)^{1-n}$ for the bottom plane. Also is for the upper plane: $\sigma_s = \sigma_m \frac{me}{ts} = \sigma_c \left(\frac{Lt}{me}\right)^n \cdot \frac{me}{ts} = \sigma_c \left(\frac{Lt}{me}\right)^{n-1} \cdot \frac{L}{s}$.

With: me = αts is: $\sigma_L = \sigma_c \left(\frac{me}{Lt}\right)^{1-n} = \sigma_c \alpha^{1-n} \left(\frac{s}{L}\right)^{1-n}$

and is: $\sigma_s = \sigma_c \alpha^{1-n} \left(\frac{L}{s}\right)^n$

In general is Eq.(A.1): $f(x) = f(x_0) \cdot \left(\frac{x}{x_0}\right)^m$, for $x = x_0 \frac{s}{L}$, equal to: $\sigma_L = \sigma_c \alpha^{1-n} \left(\frac{s}{L}\right)^{1-n}$

and for for $x = x_0 \frac{L}{s}$, equal to: $\sigma_s = \sigma_c \alpha^{1-n} \left(\frac{L}{s}\right)^n$

Because the exponent gives the slope of the curve and the curve should not be kinked at x_0, the exponents should be the same and: m = 1 - n = n, or n = 1/2.

For α =1, the intermediate plane is the determining upper plane

Literature

[1] F. Kollmann, Principles of wood science and technology, vol. I, 1984, Springer-Verlag, Berlin.

[2] T.A.C.M. van der Put, A general failure criterion for wood, Proc. IUFRO S5.02 paper 23, 1982, Boras, Sweden.

[3] H. Schwarty, PhD dissert. Stuttgart, 1969.

[4] T.A.C.M. van der Put, The tensor-polynomial failure criterion for wood polymers, www.dwsf.nl/downloads.htm, Delft, 2005.

[5] H.J. Larsen, The design of timber beams, CIB-W18/5-10-1, Karlsruhe, 1975.

[6] U. Korin, Compression perpendicular to grain, CIB-W18/23-6-1, Lisbon 1990.

[7] M. Augustin et al. Behaviour of glulam in compression perpendicular to grain in different strength grades and load configurations, CIB-W18/39-12-6, Florence, 2006.

[8] T.A.C.M van der Put, Discussion of the failure criterion for combined bending shear and compression. CIB-W18/24-6-1, Oxford, 1991.

[9] T.A.C.M van der Put, Leijten, A.J.M., Evaluation of perpendicular to the grain failure of beams by concentrated loads of joints. CIB-W18/33-7-7, NL, 2000.

[10] T.A.C.M van der Put, Explanation of the embedding strength of particle board, Stevin Report TU-Delft 25-88-63/09-HSC-6 or: EC-project MA1B-0058-NL, 1988.

[11] M. Ballerini, A new set of tests on beams loaded perpendicular to the grain by dowel joints, CIB-W18/32-7-2, Graz, Austrie, 1999.